



Wind turbine condition monitoring based on SCADA data using normal behavior models. Part 2: Application examples



Meik Schlechtingen ^{a,*}, Ilmar Ferreira Santos ^b

^a Department of Technical Operation Wind Offshore, EnBW Erneuerbare Energien GmbH, Admiralitätstr.4, 20459 Hamburg, Germany

^b Department of Mechanical Engineering, Section of Solid Mechanics, Technical University of Denmark, Denmark

ARTICLE INFO

Article history:

Received 12 September 2012

Received in revised form 11 April 2013

Accepted 24 September 2013

Available online 8 October 2013

Keywords:

ANFIS models

Condition monitoring

Wind turbine

SCADA data

Normal behavior models

ABSTRACT

This paper is part two of a two part series. The originality of part one was the proposal of a novelty approach for wind turbine supervisory control and data acquisition (SCADA) data mining for condition monitoring purposes. The novelty concerned the usage of adaptive neuro-fuzzy interference system (ANFIS) models in this context and the application of a proposed procedure to a wide range of different SCADA signals. The applicability of the set up ANFIS models for anomaly detection was proven by the achieved performance of the models. In combination with the fuzzy interference system (FIS) proposed the prediction errors provide information about the condition of the monitored components.

Part two presents application examples illustrating the efficiency of the proposed method. The work is based on continuously measured wind turbine SCADA data from 18 modern type pitch regulated wind turbines of the 2 MW class covering a period of 35 months. Several real life faults and issues in this data are analyzed and evaluated by the condition monitoring system (CMS) and the results presented. It is shown that SCADA data contain crucial information for wind turbine operators worth extracting. Using full signal reconstruction (FSRC) adaptive neuro-fuzzy interference system (ANFIS) normal behavior models (NBM) in combination with fuzzy logic (FL) a setup is developed for data mining of this information. A high degree of automation can be achieved. It is shown that FL rules established with a fault at one turbine can be applied to diagnose similar faults at other turbines automatically via the CMS proposed. A further focus in this paper lies in the process of rule optimization and adoption, allowing the expert to implement the gained knowledge in fault analysis. The fault types diagnosed here are: (1) a hydraulic oil leakage; (2) cooling system filter obstructions; (3) converter fan malfunctions; (4) anemometer offsets and (5) turbine controller malfunctions. Moreover, the graphical user interface (GUI) developed to access, analyze and visualize the data and results is presented.

© 2013 Elsevier B.V. All rights reserved.

1. Introduction

Condition monitoring of wind turbines is of increasing importance as the size and remote locations of wind turbines used nowadays makes the technical availability of the turbine very crucial. Especially offshore unexpected faults, especially of large components, can lead to excessive downtime due to the lack of suitable crane ships or other specialized vessels. However, also smaller issues and faults of auxiliary equipment like pumps or fans can cause expensive turbine downtime due to restricted turbine accessibility. From an operator's point of view, it is therefore worth increasing the effort to monitor the turbine condition in order to reduce unscheduled downtime and thus operational costs.

Typically the available condition monitoring systems (CMSs) require high-level knowledge about the system to be monitored. However, this knowledge is difficult to access and often does not exist. Physical models of the system to monitor its condition and predict failures can thus seldomly be built with high accuracy due to its complex interaction among several dynamical subsystems [1]. Moreover, the available CMSs mainly focus on vibration analysis. Vibration analysis is by far the most prevalent method for machine condition monitoring [2]. However, vibration sensors are not installed on all turbines and components due to their high costs. This leads to a large number of wind turbines not being condition monitored at all or vibration sensors being installed at the main components only.

In contrast to vibration data there is a large amount of operational (SCADA) data available, which can be used to give an indication of the turbine condition. This fact is also stressed by Yang and Jiang [3] who additionally point out that these data are the cheapest resource for developing a CMS for wind turbines.

* Corresponding author. Tel.: +49 40533268134.

E-mail address: m.schlechtingen@enbw.com (M. Schlechtingen).

In part one of this paper series [1], a CMS is proposed utilizing adaptive neuro-fuzzy interference systems (ANFIS) to build normal behavior models (NBM) based on ordinary SCADA data. The resulting prediction error pattern of the different models is further analyzed by means of fuzzy logic (FL) rules in order to extract information about the component conditions. Part two will now entirely focus on application examples illustrating the performance of the proposed CMS. More information about the reasoning for choosing ANFIS models as well as FL can be found in part one [1].

The research presented in this paper is the result of two years investigations carried out to develop a CMS that uses wind turbine SCADA data available to wind turbine operators. The data available is obtained from 18 operating onshore turbines of the 2MW class, where continuous operational data were gathered from April 2009 to March 2012.

In Section 2 of this paper the graphical user interface (GUI) developed to access and visualize the large amount of data is briefly introduced. Additionally general comments about the data volume are made and the result visualization is presented. In Section 3, a flow chart illustrates the information flow and the fuzzy rule optimization process. Examples emphasizing the working principle and the effectiveness of the proposed method are given in Section 4. Results are discussed in Section 5. Section 6 focuses on future aspects and conclusions are drawn in Section 7.

2. General comments, graphical user interface and visualization

The large amount of SCADA data available to wind turbine operators requires a systematic and standardized handling of data. For condition monitoring purposes, not all SCADA data supplied are of interest. The first difficulty therefore arises from the selection of suitable signals for processing by the proposed CMS. The number of data tags available for a 10 min period can easily exceed 1000. This includes digital values, hour counters, calculated values, set point and statistical values (mean, minimum, maximum and

standard deviation) for each 10 min period. For the reasons given in part one [1], the focus lies on 10 min average values in this research. Due to the number of data tags supplied by the turbine manufacturer, 45 models are developed for each turbine in this research covering a broad variety of signals. Thus in total 810 (45 × 18) models are developed, trained and their prediction error monitored. For systematic handling, a graphical user interface (GUI), Fig. 1, was developed that eases data access, visualization and analysis. The functionality of the different features in the GUI are:

- (A) Wind power plant selection: Allows the selection of different wind farms in the future (currently one implemented),
- (B) Turbine selection
- (C) Module selection (compare part one Fig. 1):
 - Training module: the ANFIS models are trained, or new data processed.
 - Anomaly detection module: Anomalies in the prediction error are detected.
 - Fuzzy expert module: evaluates existing rules and stores the results for graphical visualization.
- (D) Retrain panel: When the signal behavior changes due to service or replaced/repaired components, retraining of the models may be required, which can be controlled in this panel.
- (E) Advanced settings: Training and preprocessing settings can be edited to assure proper model performance
 - Maximum signal lag to be removed before modeling
 - Minimum turbine power output for analysis
 - Filtering of transient situations, e.g. after turbine start
 - Number of data days and turbine operational days for the different training states
 - Probability value giving the alarm limits
 - Number of days the anomaly detection module shall wait for a reoccurring anomaly before forgetting
 - Number of values to average (here 144 values equal to one day is chosen)
- (F) Signal selection
- (G) Signal selection
- (H) Signal selection
- (I) Signal selection
- (J) Signal selection
- (K) Signal selection

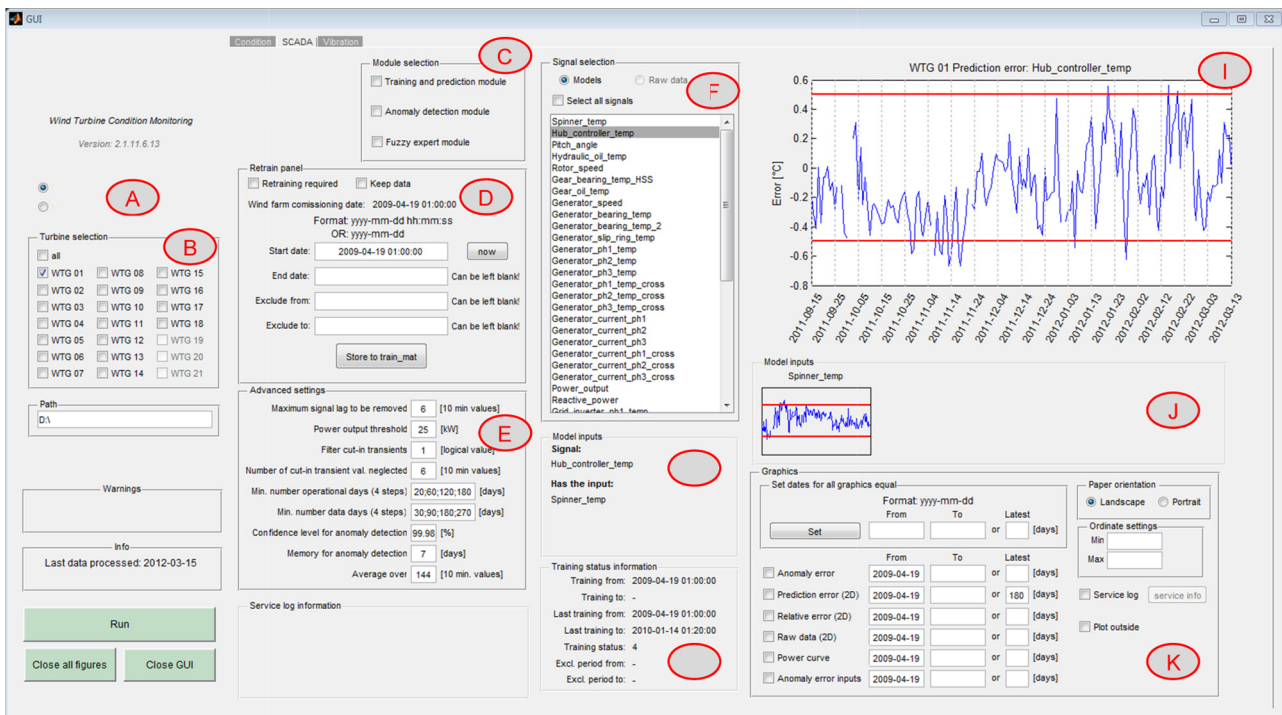


Fig. 1. GUI.

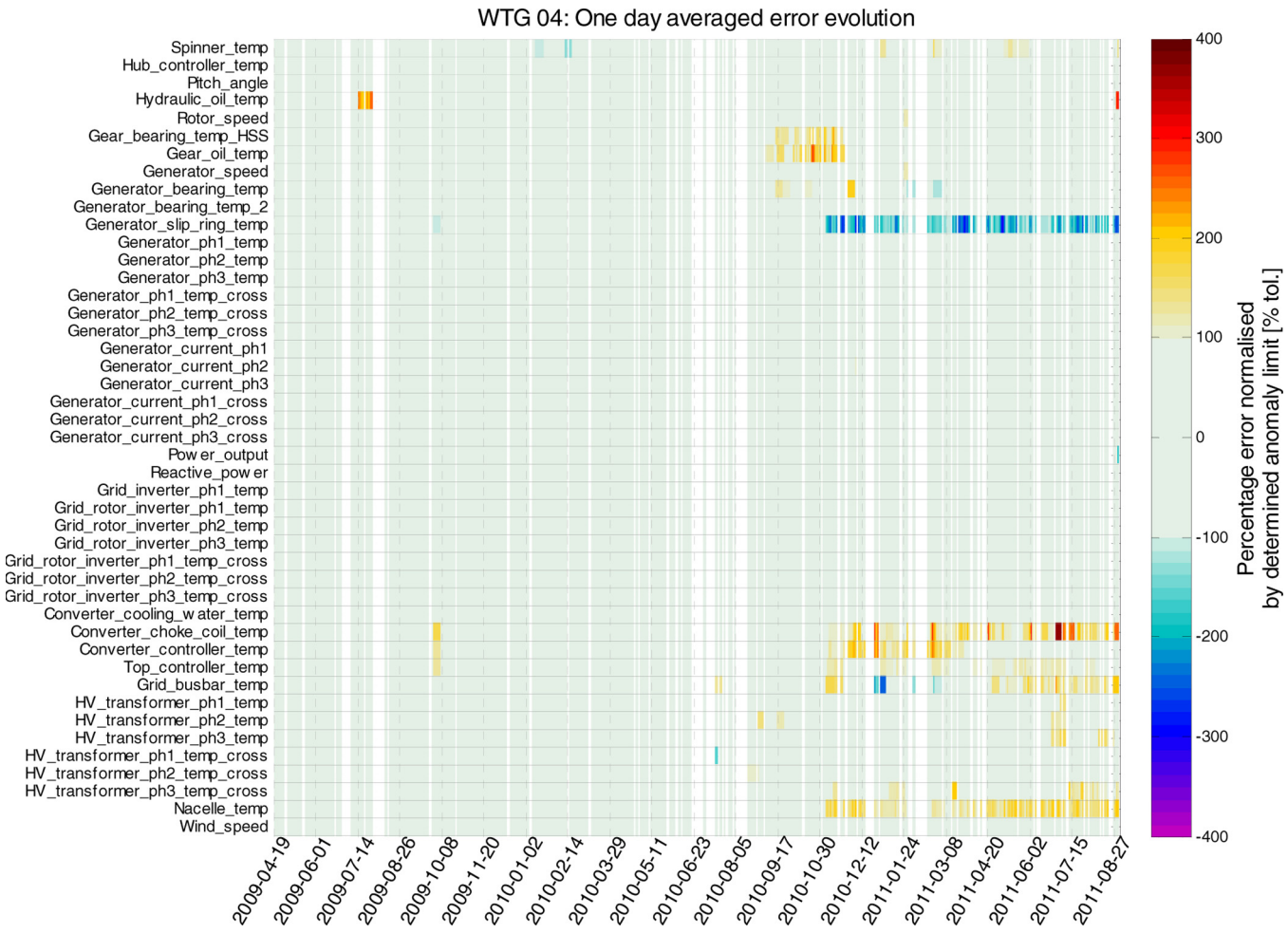


Fig. 2. Percentage error normalized by the determined alarm limit (WTG 04).

- (G) Normal Behavior Model (NBM) input information: Gives information about which input signals are used to build the particular model
- (H) Training status information: Training states (one to four) according to the steps defined in the advanced settings panel
- (I) One day average prediction error visualization: Visualization of the prediction error of the selected signal
- (J) One day average model inputs prediction error visualization: Helping the expert to find the root cause of prediction error deviation from normal (only displayed, when NBM for specific input exists)
- (K) Different graphic settings used for analysis:
 - Anomaly error to get a quick overview about the prediction errors of the selected signals
 - 2D prediction error to visualize the prediction error magnitude
 - Relative error as being the prediction error divided by the actual measurement in this period
 - Raw data
 - Wind turbine power curve
 - Anomaly error inputs showing the prediction error evolution over time of the model inputs and the output

Using the anomaly error plot function of the GUI (see area K in Fig. 1) the model error of all developed and monitored models per wind turbine can be visualized to get an overview of current model deviations. For this purpose the predictions errors are normalized by the determined anomaly limit. In Fig. 2 a 2D waterfall plot of

the normalized averaged percentage prediction errors over time is visualized for WTG 04 to emphasize the strength of this illustration in getting a one shot overview about present model deviations.

In this plot the colors indicate the prediction error amplitude. White areas mark periods where no prediction is available, e.g. due to missing data or non-operational periods. A wind turbine schematic is visualized in Fig. 3.

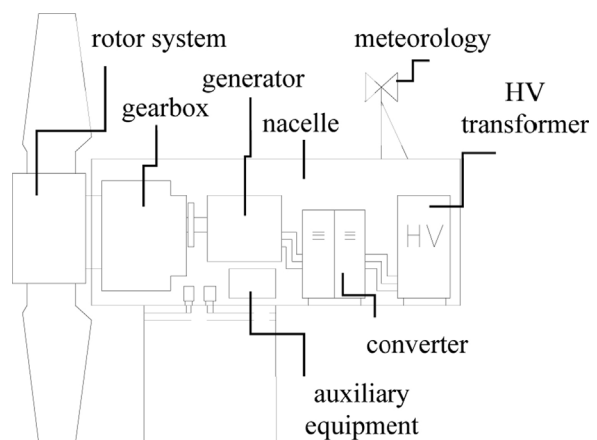


Fig. 3. Wind turbine schematic: components/subsystems in the considered wind turbines.

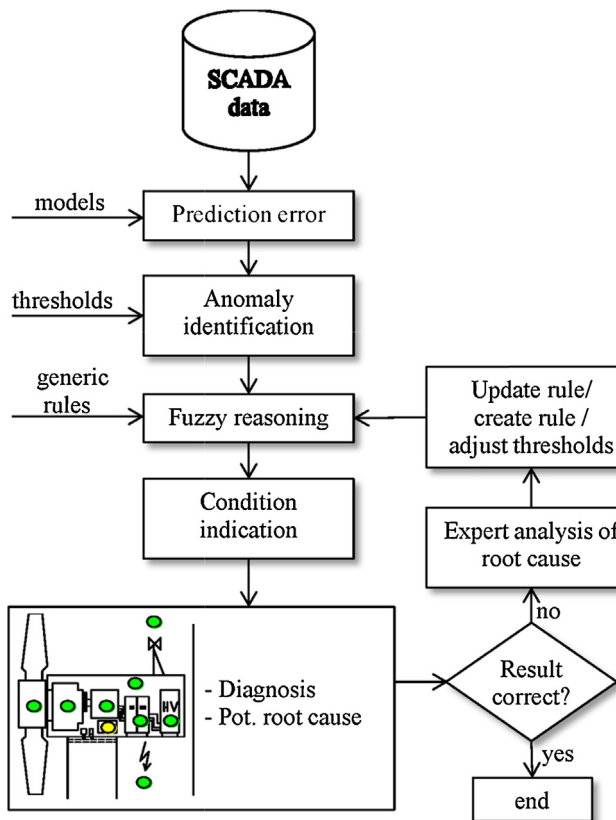


Fig. 4. Information flow.

3. Information flow

In order to arrive at component condition statements FL rules must be implemented by an expert who is familiar with the behavior of the turbine, typical faults and their root causes. There are two types of rules

- generic rules
- specific rules

The generic rules are used to highlight present anomalies, in case no specific rule applies. This rule type gives no information about the specific condition or potential root cause, but highlights anomalies in the data. The specific rules on the other hand provide this level of information [1]. The overall information flow and diagnosis optimization loop is emphasized in Fig. 4.

The expert analysis of the root cause is aided by the prediction errors, the raw data, service protocols, on-site inspections and personal experience. Once the root cause is identified, the generic rule can be updated, or a specific rule implemented that captures the fault pattern and leads to a correct diagnosis. Moreover, the thresholds defining anomalies can be adjusted by the expert to give a better indication of the actual component condition, i.e. make the system more sensitive or less sensitive. In this fashion, the expert system will become more diverse over time concerning different diagnoses and more precise in condition classification. More information about the fuzzy expert system can be found in part one [1].

Next, a number of examples will be presented which show the rule implementation process in more detail, followed by examples showing the system performance and general rule application.

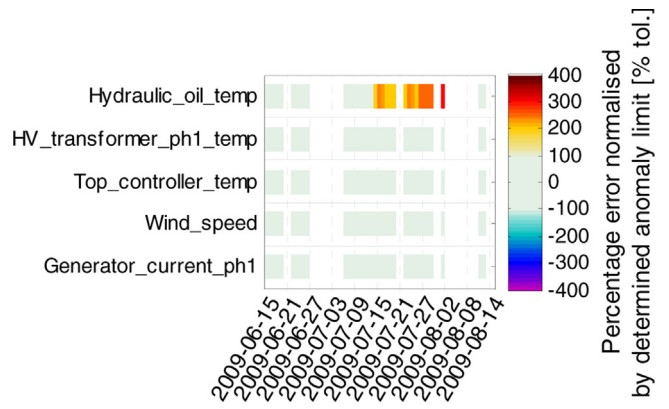


Fig. 5. Normalized prediction errors of the hydraulic oil temperature and related inputs (WTG 04).

4. Examples

The examples given in this section are real measured faults analyzed by the proposed CMS. Note that during CMS development no monitoring was performed, i.e. the examples given here are based on re-analysis.

4.1. Example 1: Hydraulic oil leakage

In the first example, an anomaly in hydraulic oil temperature is highlighted by the CMS developed. In addition to this, it is emphasized how information about the anomaly root cause can be implemented in the CMS in order to ease the analysis of future faults. Fig. 5 shows a 2D waterfall plot of the normalized averaged percentage prediction errors of the hydraulic oil temperature and the related inputs of the NBM over time. Figure was generated by selecting the period between 2009-06-15 and 2009-08-14 and the anomaly error inputs graphic setting.

It is visible that beginning on 2009-07-16 an anomaly with rising amplitude occurs in the prediction error of the hydraulic oil temperature. At the same time, the related inputs behave normal, which points to a real anomaly in the hydraulic oil temperature data.

Fig. 6 shows the prediction error and Fig. 7 the raw time series of the hydraulic oil temperature during anomaly occurrence over time to point out the amplitude height of the prediction error during fault occurrence.

The trend in the prediction error is clearly visible. The highest prediction error peak is around 15 °C. Although the raw time series also indicates a trend, its visibility is dependent on the operational mode of the turbine.

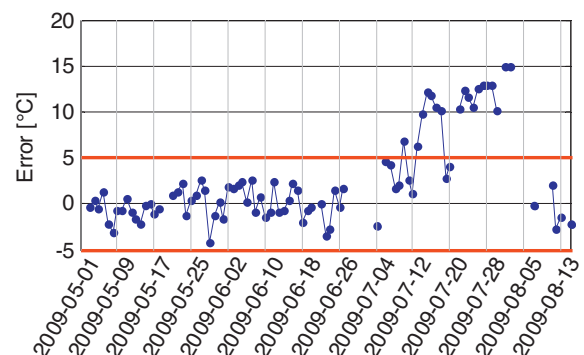


Fig. 6. Hydraulic oil temperature prediction error and anomaly limits (WTG 04).

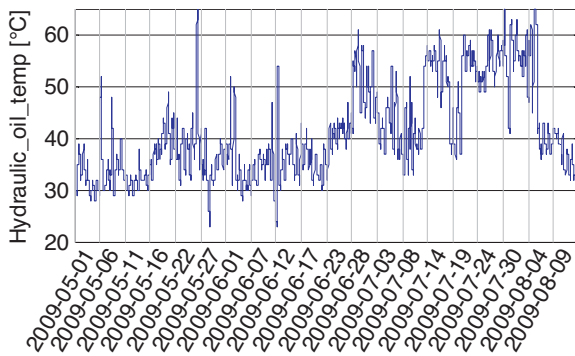


Fig. 7. Hydraulic oil temperature raw time series (WTG 04).

The anomaly pattern of the normalized prediction error is analyzed by the fuzzy expert application module and a high hydraulic oil temperature is highlighted on 2009-07-16 by the CMS via the following generic rule:

If (Anomaly error (5 MFs) Hydraulic oil temp.==high/very high) & (Anomaly error (3 MFs) HV transformer ph.1 temp.==ok) & (Anomaly error (3 MFs) Top controller temp.==ok) & (Anomaly error (3 MFs) Generator current ph.1==ok) & (Anomaly error (3 MFs) Nacelle temp.==ok) **then** (Diagnosis==Hydraulic oil temp. high) (Condition==yellow/red)(Pot. root cause==Ambiguous)

These initial generic rules give no information about the potential root cause. The condition statements “yellow” and “red” are based on the general anomaly definition given in part one [1]. The fault can now be investigated and a rule established based on the diagnosed root cause. In this specific case, the root cause was a leakage in the rotary joint, causing the oil pump to run permanently and thus heating up the oil. The entries in the service report were used to set up the specific rules containing the expert knowledge as follows.

If (Anomaly error (5 MFs) Hydraulic oil temp.==high/very high) & (Anomaly error (3 MFs) HV transformer ph.1 temp.==ok) & (Anomaly error (3 MFs) Top controller temp.==ok) & (Anomaly error (3 MFs) Generator current ph.1==ok) & (Anomaly error (3 MFs) Nacelle temp.==ok) **then** (Diagnosis==Hydraulic oil temp. high)(Condition==yellow/red)(**Pot. root cause==Pump running permanently, leakage possible**)

The terms high “yellow” and very high “red” of the hydraulic oil temperature prediction error are defined in a master threshold table with 5 °C and 14 °C respectively, to reflect the gained knowledge of the component condition. Repair took place on 2009-08-06. Reanalyzing the fault gives the results presented in Table 1.

The expert knowledge was successfully implemented and the CMS is now able to identify and diagnose similar issues on other turbines of the fleet. It is worth noting, that the generic rules can be set up before fault occurrence based on general engineering knowledge about the system behavior in fault situations. While each turbine

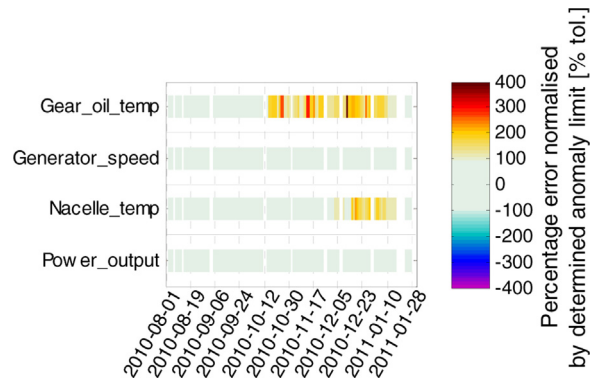


Fig. 8. Normalized prediction errors of the gearbox oil temperature and related inputs (WTG 10).

is treated individually with respect to the NBMs, the implemented rules are applicable for all turbines of the same type, which is shown in the next examples.

4.2. Example 2: Gearbox oil temperature increase A

The second example shows an increase in gearbox oil temperature due to dirty filters of the cooling system. Again, a 2D waterfall plot is used to emphasize present anomaly patterns (see Fig. 8).

It is visible that the gearbox oil temperature deviates from normal behavior round 2010-10-15, while all inputs are normal. At 2010-11-31 the input nacelle temperature leaves normal behavior and indicates a positive deviation, i.e. higher nacelle temperatures. This effect is a consequence resulting from the increased gearbox temperature, as the gearbox together with the generator are the main heat sources in the nacelle. Consequentially a higher gearbox temperature leads to a higher nacelle temperature. The prediction error magnitude and the anomaly limits of the gearbox oil temperature are visualized in Fig. 9 and the corresponding raw time series in Fig. 10.

The fluctuating pattern of the prediction error is typical for the deviation from normal behavior being depended on the turbine power output, i.e. high prediction error when high efficiency of the cooling system is required (full load) and low when the turbine power output is low. To some extent, this makes the correct classification into the category yellow and red depended on the power output. However, this can be overcome, if only the worst condition is considered until the component condition falls back to normal (green).

The raw data do indicate an increase in temperature, but the level of increase appears to be constant beyond mid-August.

The increase in gearbox oil temperature is highlighted by the CMS at 2010-10-15 via the generic rules:

If (Anomaly error (5 MFs) Gearbox oil temperature temp.==high/very high) & (Anomaly error (3 MFs) Generator

Table 1
Turbine condition evolution during hydraulic oil leakage occurrence (WTG 04).

2009-07-15	2009-07-16	2009-08-01	2009-08-11
Component working as expected None	Hydraulic oil temp. too high Pump running permanently, leakage possible	Hydraulic oil temp. too high Pump running permanently, leakage possible	Component working as expected None

Table 2

Turbine condition evolution during filter pollution (WTG 10).

2010-10-14	2010-10-15	2010-12-11	2010-01-12

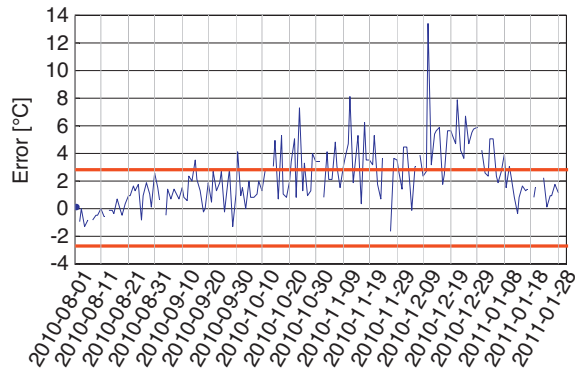
Component working as expected
NoneGearbox oil temp. too high
AmbiguousNo rule applicable
AmbiguousComponent working as expected
None

Fig. 9. Gear oil temperature prediction error and anomaly limits (WTG 10).

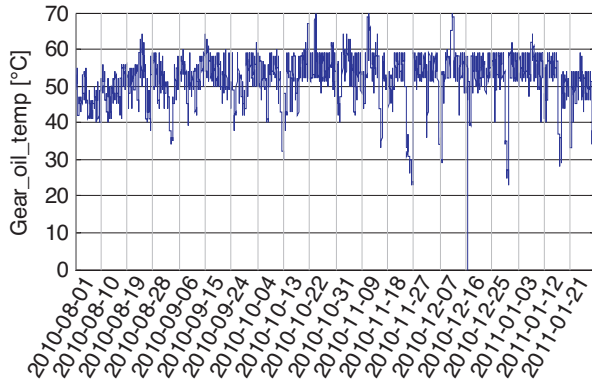


Fig. 10. Gear oil temperature raw time series (WTG 10).

speed==ok) & (Anomaly error (3 MFs) Nacelle temp.==ok) & (Anomaly error (3 MFs) Power output==ok) **then** (Diagnosis==Gearbox oil temp. high) (Condition==yellow/red) (Pot. root cause==Ambiguous)

Table 3

Turbine condition evolution during filter pollution (WTG 10).

2010-10-14	2010-10-15	2010-12-11	2010-01-12

Component working as expected
NoneGearbox oil temp. too high
Cooling insufficient, filter pollutedGearbox oil temp. too high
Cooling insufficient, filter pollutedComponent working as expected
None

The categorization into the condition category “yellow” takes place based on the standard definitions of anomaly. The condition evaluation is summarized in Table 2.

At 2010-12-11 the gearbox condition turned to “grey” (no diagnosis possible), as no rule in the rule base reflected the present pattern. This is because the generic rule requires the nacelle temperature to be normal. However, at 2010-12-11 the nacelle temperature model did also show a high prediction error, which prevented the generic rule from firing. This temperature increase is because of the physical link of the gearbox temperature and nacelle temperature. Note that during the increase in gearbox oil temperature no automatic diagnosis of the nacelle temperature can take place (indicated by the gray dot).

The service protocol reveals that the six months service was performed on the 2011-01-12 and the maintenance manual indicates that the filter was replaced, causing the normalization of the prediction error. Knowing this, the generic rules can be changed into specific rules with regards to the potential root cause and the general rule setup.

If (Anomaly error (5 MFs) Gearbox oil temperature temp.==high/very high) & (Anomaly error (3 MFs) Generator speed==ok) & (Anomaly error (3 MFs) Nacelle temp.~==low) & (Anomaly error (3 MFs) Power output==ok) **then** (Diagnosis==Gearbox oil temp. high) (Condition==yellow/red) (**Pot. root cause==Cooling insufficient, filter polluted**)

Additionally the threshold for the condition “red” was changed to 10°C in the master threshold table, in order to make condition statements equal for all turbines and to better reflect the pollution status. Reanalyzing the prediction error evolution gives the correct results as stated in Table 3.

The filter pollution is a frequent phenomenon at this type of turbine, which allows a check of rule validity for other turbines. This check is done in the next example.

4.3. Example 3: Gearbox oil temperature increase B-G

In this example the specific rules implemented in example 2, are applied to the same issue at other turbines. Fig. 11 shows the 2D waterfall plot during filter pollution at WTG 09.

Table 4

Turbine condition evolution during gearbox oil temperature increase due to filter pollution (WTG 09).

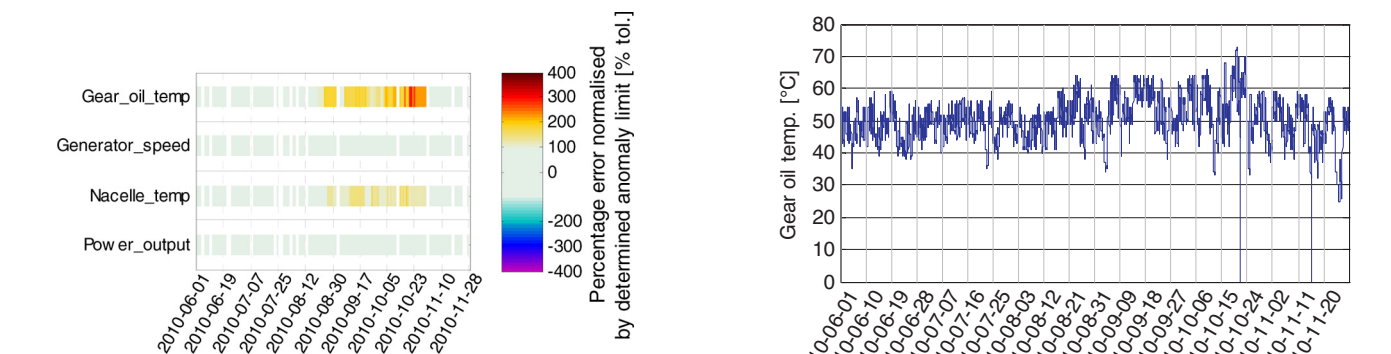
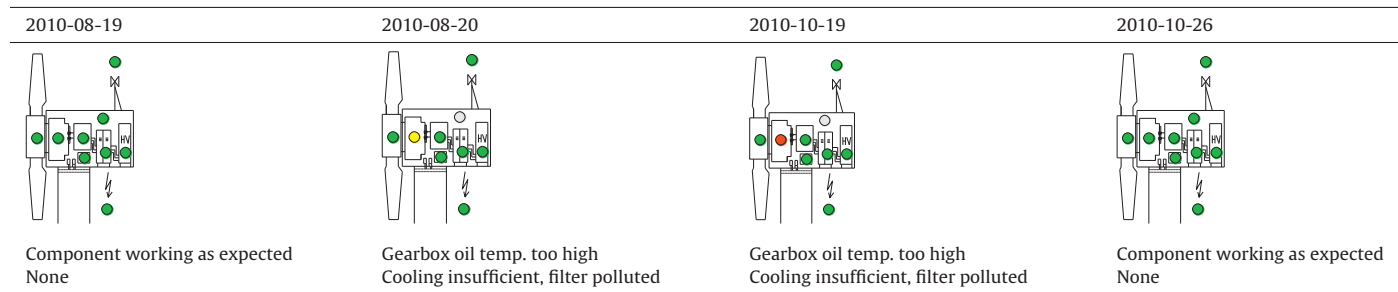


Fig. 11. Normalized prediction errors of the gearbox oil temperature and related inputs (WTG 09).

The first anomaly in gear oil temperature occurs at 2010-08-20. Six days later the nacelle temperature leaves the normal operational range. Fig. 12 shows the prediction error amplitudes and Fig. 13 the raw time series of the gearbox oil temperature during filter pollution.

Although the temperature deviation from normal behavior is up to 11°C the increase was not highlighted by the turbine controller, due to usually high thresholds set. After filter replacement the temperature fell back to the normal operational range.

The trend is also visible in the raw time series, but the fluctuations due to the different operational modes make it more difficult to identify the anomaly. Note that setting simple thresholds to the raw signal would make the identification of the increase dependent on the operational mode. A partially loaded turbine would thus delay the fault discovery, which shows the effectiveness of the proposed method.

The evolution of the gearbox condition during filter degradation is visualized in Table 4. The filter was replaced on 2010-10-25.

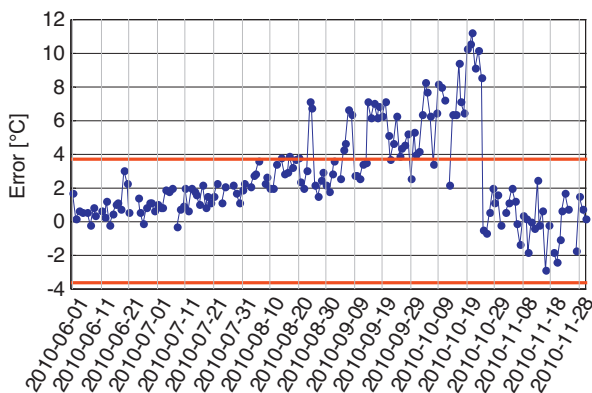


Fig. 12. Gear oil temperature prediction error and anomaly limits (WTG 09).

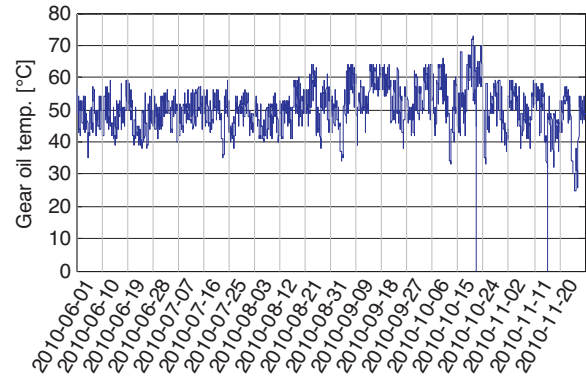


Fig. 13. Gear oil temperature raw time series (WTG 09).

The condition was correctly classified. There were six other turbines detected with the same root cause. The result of the condition evaluation is presented in Table 5 and the corresponding prediction errors of the gearbox oil temperature in Fig. 14. The pattern present between the different turbines is similar. The set threshold for the condition category "red" (10°C) is acceptable as this category should be used only when action is required.

It should be noted that although each turbine is treated individually with regards to the signal behavior (each turbine has its own model and model accuracy) the categorization into the condition categories is possible. Due to the different model accuracies the category "yellow" is different for each turbine, since it has not been defined in the master threshold table.

4.4. Example 4: Converter fan malfunction A

Modern type wind turbines operate at variable speed. In order to be able to connect to the grid, a stable frequency is required, equal to the grid frequency.

In wind turbines, this is achieved via a frequency converter (AC-DC-AC). It is thus a central component of the turbine, without which no power can be supplied. In following example, a relay failure caused the converter cabinet temperature to increase, since the fan was not working. The cabinet temperature is not available at this type of turbine, but the component temperature increase

Table 5

Condition evaluation summary for the polluted filter phenomenon.

WTG	Yellow	Red	Filter change	Max div.
02	2010-08-24	2010-10-19	2010-11-23	15°C
06	2010-09-14	–	2010-10-15	5.8°C
12	2010-09-08	–	2010-11-17	7.8°C
14	2010-07-15	2010-10-01	2010-11-10	13.1°C
17	2010-10-17	–	2011-01-28	8.1°C
18	2010-08-23	–	2010-10-12	6.6°C

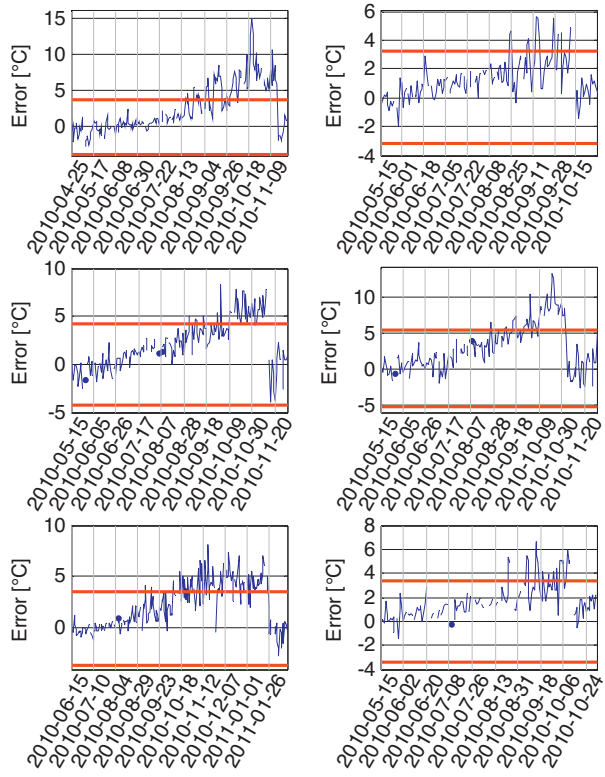


Fig. 14. Prediction errors during filter pollution (from top left to bottom right): WTG 02, WTG 06, WTG 12, WTG 14, WTG 17 and WTG 18.

can be identified at the converter choke coil and the converter controller, mounted in the converter cabinet. Fig. 15 shows the 2D waterfall plot of the converter choke coil temperature and the related inputs and Fig. 16 analogously a similar plot of the converter controller temperature.

Both models show a positive model deviation, while the related inputs to the models behave normal. Note that due to the different thresholds for the models the anomaly is pronounced differently, i.e. the percentage error normalized is higher for the controller temperature because the model is more accurate. Figs. 17 and 18 show the prediction error evolution of the two temperatures, and Figs. 19 and 20 the raw time series.

In the prediction errors, the anomalies are clearly visible, while they are practically invisible in the raw time series. At 2010-05-07 the turbine had an error due to high temperature of the top controller (master controller in the nacelle from which all the turbine subsystems are controlled and monitored).

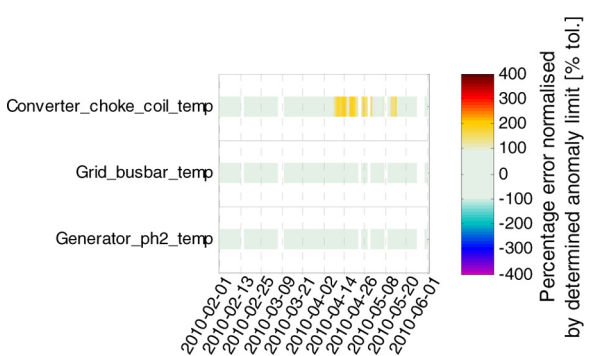


Fig. 15. Normalized prediction errors of the converter choke coil temperature and related inputs (WTG 14).

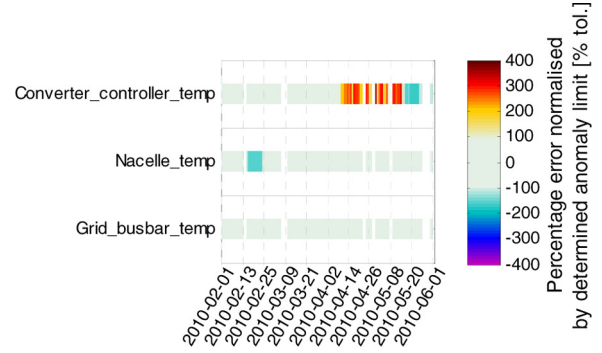


Fig. 16. Normalized prediction errors of the converter controller temperature and related inputs (WTG 14).

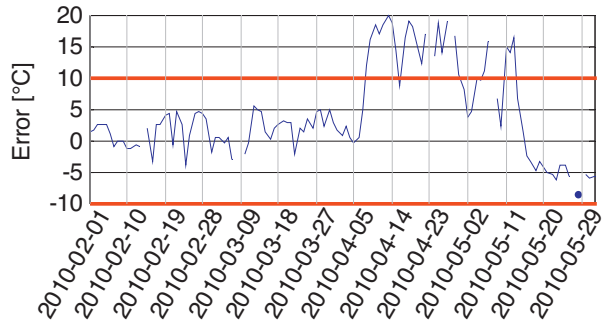


Fig. 17. Prediction error converter choke coil temperature WTG 14.

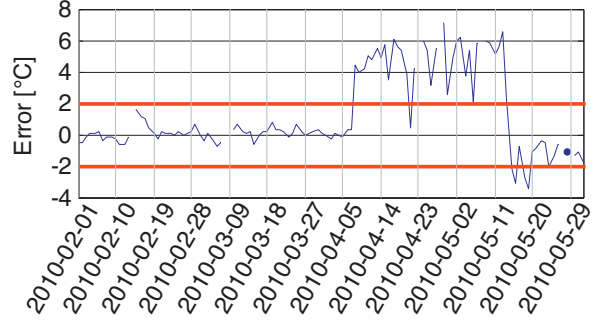


Fig. 18. Prediction error converter controller temperature WTG 14.

The turbine restarted based on auto reset one hour later. However, due to dying wind speeds the error did not occur again until 2010-05-11 where the turbine was shut down for 6 hours. One day later the error triggered the third time and a service team was sent

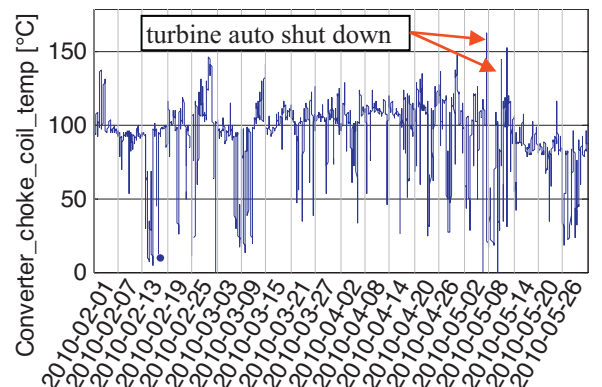


Fig. 19. Raw time series of the converter choke coil temperature WTG 14.

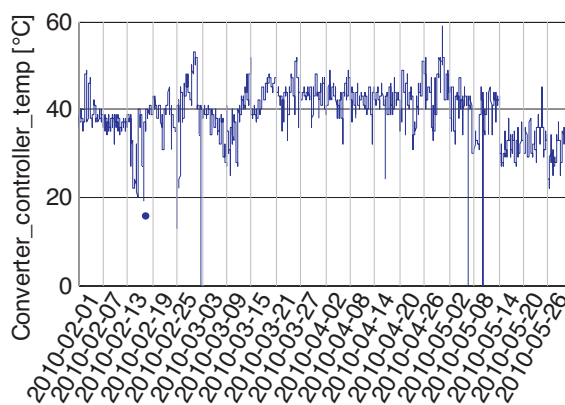


Fig. 20. Raw time series of the converter choke coil temperature WTG 14.

Table 6

Turbine condition evolution during fan malfunction increase due to dirty filters (WTG 14).

2010-04-07	2010-04-08	2010-05-13
Component working as expected None	Converter choke coil temp. high Ambiguous	Component working as expected None

out and identified the root cause to be a defective relay. Another seven hours of turbine downtime were generated.

The two temperatures considered here by the CMS belong to the same component “Converter”.

Initially there were four generic rules established to highlight anomalies in the prediction error. They were:

If (Anomaly error (5 MFs) Converter choke coil temp.==high/very high) & (Anomaly error (3 MFs) Grid busbar temp.==ok) & (Anomaly error (3 MFs) Generator ph.2 temp.==ok) **then** (Diagnosis==Converter choke coil temp. high) (Condition==yellow/red) (Pot. root cause==Ambiguous)

If (Anomaly error (5 MFs) Converter controller temp.==high/very high) & (Anomaly error (3 MFs) Nacelle temp.==ok) & (Anomaly error (3 MFs) Grid busbar temp.==ok) **then** (Diagnosis==Converter controller temp. high) (Condition==yellow/red) (Pot. root cause==Ambiguous)

Since both temperatures behave abnormal during this fault and only one condition can be assigned to the component the rules must be weighted in order to track the right root cause. Since the

Table 8

Condition evaluation summary for the polluted filter phenomenon.

WTG	Yellow	Red	Issue resolved	Max div.
03	2010-05-22	2010-11-28	2011-01-11	40.2 °C
08	2010-12-19	2011-01-15	2011-04-13	25.0 °C
12	2009-09-10	–	2009-10-07	13.1 °C
18	2010-11-08	2010-12-21	2011-04-13	38.8 °C

converter choke coil temperature level is much higher than the temperature level of the converter controller, heat is transferred from the choke coil to the controller. Hence, in case both temperatures show an increase, it is more likely that the choke coil is the cause, as an increase in controller temperature is unlikely to be noticed in the choke coil temperature. For this reason, the weights of the rules treating the converter controller temperature were set to 0.9, whereas the weights of the rules treating the converter choke coil temperature were kept by 1. [Table 6](#) summarizes the CMS result.

The condition category “red” was not triggered during fault occurrence, which is caused by the high alarm limits and the comparably inaccurate converter choke coil temperature model (the threshold for “red” lies about 30 °C).

The gained knowledge can be implemented in terms of specific rules: **If** (Anomaly error (5 MFs) Converter choke coil temp.==high/very high) & (Anomaly error (3 MFs) Grid busbar temp.==ok) & (**Anomaly error (3 MFs) Converter controller temp.==high**) & (Anomaly error (3 MFs) Generator ph.2 temp.==ok) **then** (Diagnosis==Converter choke coil temp. high) (Condition==yellow/red) (**Pot. root cause==Internal VCS fan not working/cooling insufficient**)

Based on the experienced fault pattern and the prediction error evolution, the threshold for the condition category “red” was changed to 15 °C in the master threshold table. Reanalyzing the fault gives the result presented in [Table 7](#).

The period in which the category “yellow” is active is only one day. This is acceptable, since the temperature increase is sharp and a temperature increase of 15 °C is considered serious and should initiate investigation.

4.5. Example 5: Converter fan malfunction B, C, D and E

Using the same rules further converter fan malfunctions were diagnosed by the CMS at four other turbines. The condition evaluation is summarized in [Table 8](#). [Fig. 21](#) shows the relevant prediction errors during anomaly occurrence.

Even though the turbine shuts down when a high temperature is detected, the turbine restarts automatically, usually two times before the auto restart is suppressed. Latest after the third time of high temperature, a service action is required to resolve the issue. Using the proposed CMS the issue can be detected right away. The time until a service action is required and the turbine no longer

Table 7

Turbine condition evolution during fan malfunction (WTG 14).

2010-04-07	2010-04-08	2010-04-09	2010-05-13
Component working as expected None	Converter choke coil temp. high Internal VCS fan not working/cooling insufficient	Converter choke coil temp. high Internal VCS fan not working/cooling insufficient	Component working as expected None

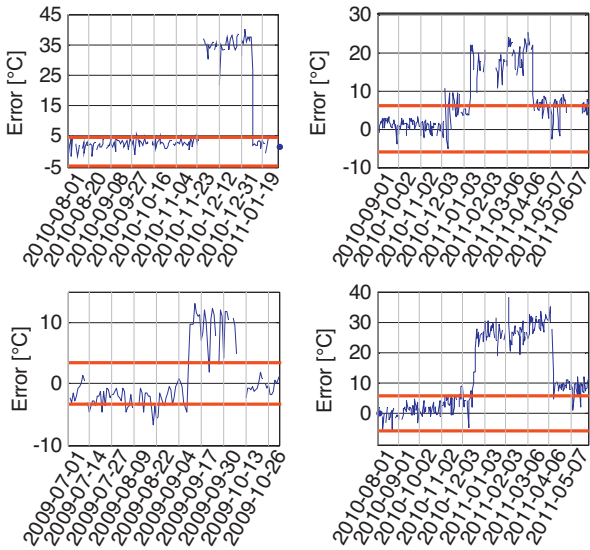


Fig. 21. Prediction errors of the converter choke coil temperature during converter malfunction (from top left to bottom right): WTG 03, WTG 08; WTG 12; WTG 18.

auto restarting can range between one to eight months (for the examples given here).

For WTG 18 the temperature level after the fan was replaced does not fall back to its normal range. This can be either due to a different setting of the thermostat, a lasting damage of the choke coil or a different fan being used. Fig. 22 illustrates the raw time series of the converter choke coil temperature, indicating the maximum temperatures during fan malfunction and the temperature level after fan replacement.

The maximum temperature of 150 °C occurred can cause the insulation of the coil to age faster, reducing the overall component live time. In order to not trigger alarms permanently, the condition thresholds for this particular turbine can be adopted to account for the persistent offset. A different approach would be to retrain the model, or to establish an offset in the prediction error. However, the latter bears the disadvantage of tracking the established offsets. Furthermore, the prediction error appears to be normal although degradation is present. The same is true for retraining in those situations. Hence, the preferred method is the adjustment of thresholds. Note that the permanent offset in choke coil temperature can influence other models, which use this signal as input.

Another interesting issue arising from Fig. 21 in combination with Table 8 is that for WTG 03 the CMS highlights the category “yellow” at 2010-05-22. However, the hard boundaries (red lines) are

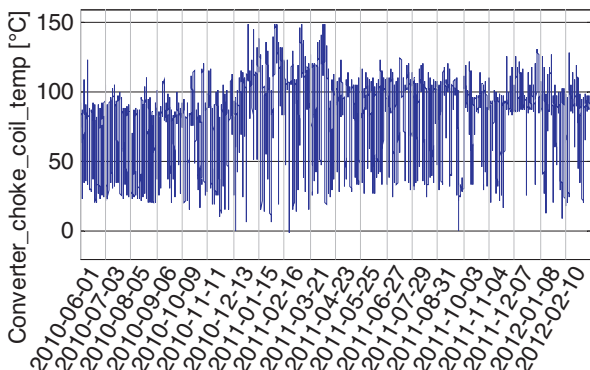


Fig. 22. Raw time series of the converter choke coil temperature (WTG 18).

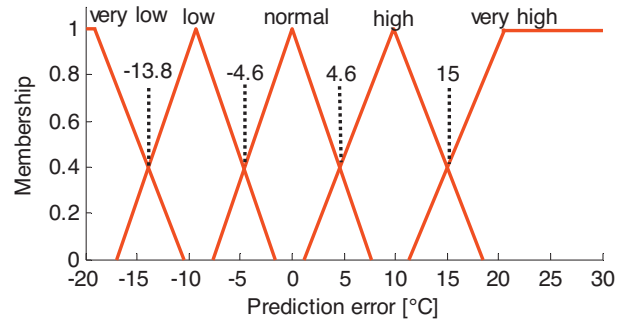


Fig. 23. Converter choke coil membership functions for the converter FIS (WTG 03).

not violated before the step increase (2010-11-28). Here the advantage of using FL instead of crisp logic becomes visible. Due to the overlap in MFs, diagnosis is still possible, although in a crisp sense the temperature still behaves normal (within the boundaries).

Fig. 23 illustrates the converter choke coil MFs for the converter fuzzy interference system (FIS), including the thresholds for condition evaluation.

The prediction error prior 2010-11-28 is just below 4.6 °C. At this prediction error level the MF “high” already contributes some membership larger than zero to the evaluation of rules. Since at this time already the converter controller temperature is abnormal (see Fig. 24), the rule highlighting the issue fires.

4.6. Example 6: Anemometer offsets

In this examples anemometer offsets are detected at all turbines. Anemometers are used to determine the cut-in and in some cases, also the cut-out wind speed. However, the information coming from the anemometers is useful for the overall turbine performance evaluation in terms of the wind turbine power curve, i.e. the turbine power output over the wind speed.

A typical power curve of a pitch regulated wind turbine is shown in Fig. 25.

As illustrated in Fig. 25, the power curve can be divided into five regions:

- Wind speed < cut in speed—the cut in speed is the wind speed value at which the turbine starts operating; power output zero or negative; pitch angle about 90°.
- Wind speed > cut in speed < rated speed; Pitch angle between 0 and –5°.
- Wind speed around rated speed; Pitch angle between –5 and 5°.
- Wind speed > rated speed; Pitch angle between 5 and 25°.

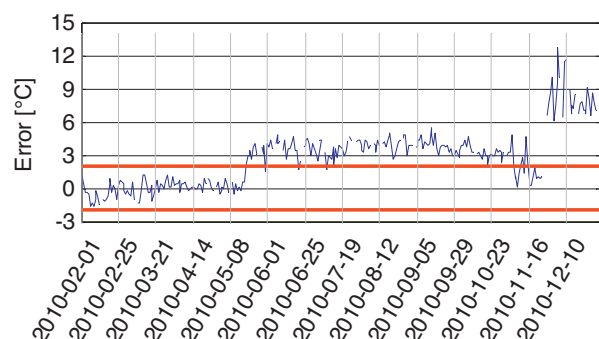
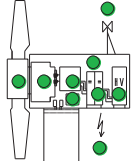
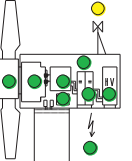
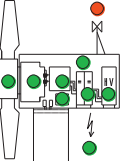
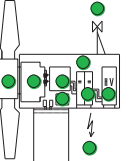


Fig. 24. Prediction error of the converter controller temperature during fan malfunction.

Table 9

Turbine condition evolution during anemometer offset (WTG 14).

2010-12-13	2010-12-14	2010-12-19	2010-12-25
			

Component working as expected
None

Wind speed measured too low
Ambiguous

Wind speed measured too low
Ambiguous

Component working as expected
None

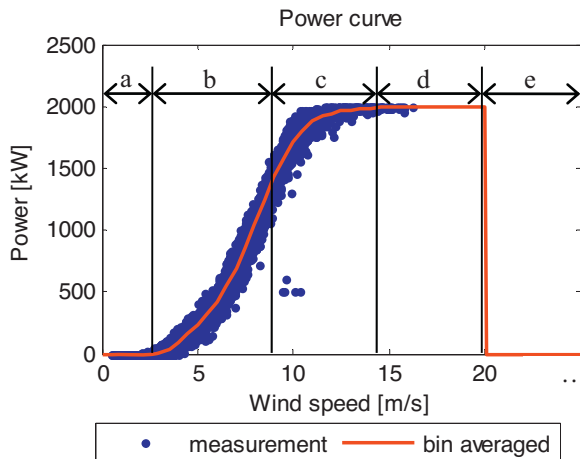


Fig. 25. Power curve properties.

(e) Wind speed > cut-out speed; power output zero or negative; pitch angle about 90°.

More information about general power curve properties can be found in Schlechtingen, Santos and Achiche [8]. If the wind speed is measured incorrect, secondary performance evaluation via the power curve is impossible or leads to wrong results. Hence, it is important to track, if the wind speeds measured fit to the measured power. Fig. 26 shows the normalized prediction errors of the wind speed and the related inputs of WTG 01 exemplary and Fig. 27 the wind speed prediction error during offset occurrence.

The wind speed prediction error shows a negative deviation, whereas the power output shows a positive deviation at the same time. This correlation is caused by the fact that these two models use each other's signal as input, i.e. the wind speed model uses the power output and the power output the wind speed as input.

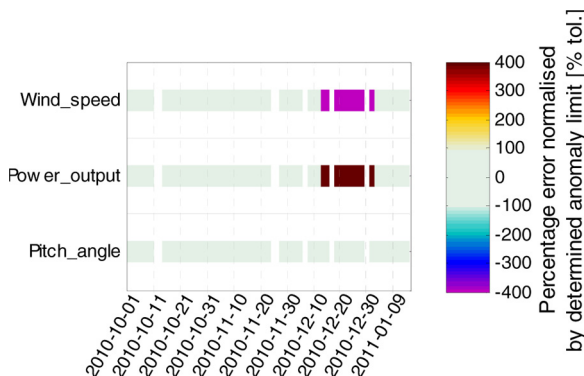


Fig. 26. Normalized prediction errors of the wind speed and related inputs (WTG 01).

This leads to the non-ideal situation, that in case of anomaly, both models will show abnormal prediction errors. However, given the set of available possible input variables, this could not be avoided.

Taking into account that a positive power output prediction error means a better than normal turbine performance the root cause can be identified, as this appears less likely than a performance decrease with lower power output. On the other hand, a positive wind speed model deviation would mean a higher wind speed measurement than usual, which in terms of a classical cup anemometer appears unlikely, too. Hence the generic rules to identify the likely cause of anomaly are:

If (Anomaly error (5 MFs) Wind speed==low/very low) & (Anomaly error (3 MFs) power output==high) & (Anomaly error (3 MFs) pitch angle==ok) **then** (Diagnosis==Wind speed measured too low) (Condition==yellow/red) (Pot. root cause==Ambiguous)

If (Anomaly error (5 MFs) power output==low/very low) & (Anomaly error (3 MFs) Wind speed~==low) & (Anomaly error (3 MFs) pitch angle==ok) **then** (Diagnosis==Power output too low) (Condition==yellow/red) (Pot. root cause==Ambiguous)

Applying these two rules, the CMS gives the result presented in Table 9.

The cause of anomaly was an offset set initiated by a software update mid-December 2010. The offset was about -0.7 m/s . The issue was also highlighted at the other turbines as summarized in Table 10.

At WTG 02 and WTG 18, no diagnosis was possible, as the wind direction signal was implausible after the software update. This made power output predictions impossible. In turn, the rules involving the power output predictions could not be evaluated. In order to account for the offset, all models taking the wind speed as input as well as the wind speed model itself were retrained, since removal of the offset could not be forced.

4.7. Example 7: Turbine controller malfunction

The last example shows a turbine master controller malfunction during which a dynamical set point caused the turbine power

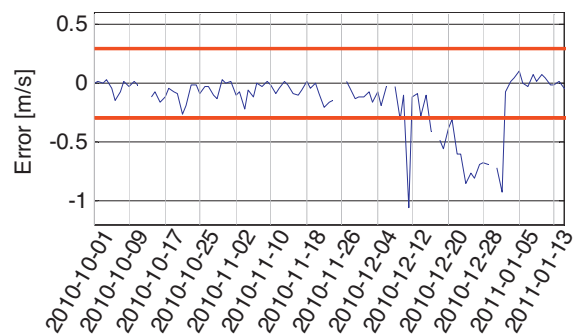
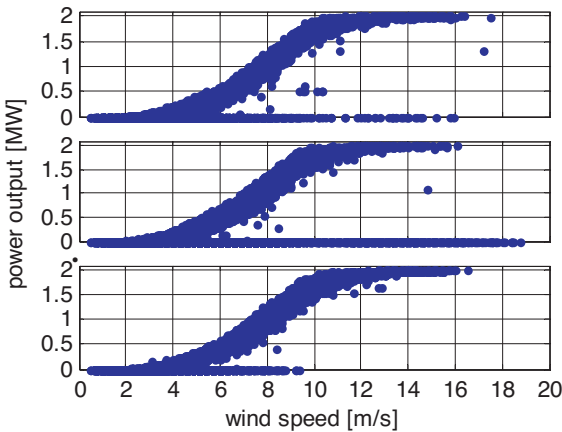


Fig. 27. Wind speed prediction error during offset occurrence (WTG 01).

Table 10

Condition evaluation summary during anemometer offset.

WTG	Yellow	Red	Retraining	Max div.
02	–	–	2010-12-25	-1.1 m/s
03	–	2010-12-19	2010-12-25	-1.1 m/s
04	2010-12-22	2010-12-24	2010-12-25	-0.9 m/s
05	–	2010-12-19	2010-12-25	-1.0 m/s
06	2010-12-18	2010-12-24	2010-12-25	-0.9 m/s
07	2010-12-19	2010-12-24	2010-12-25	-0.7 m/s
08	2010-12-20	2010-12-22	2010-12-25	-0.8 m/s
09	–	2010-12-18	2010-12-25	-0.8 m/s
10	–	2010-12-16	2010-12-25	-0.8 m/s
11	2010-12-14	2010-12-15	2010-12-25	-1.0 m/s
12	–	2010-12-19	2010-12-25	-1.0 m/s
13	–	2010-12-16	2010-12-25	-1.8 m/s
14	2010-12-18	2010-12-24	2010-12-25	-0.9 m/s
15	–	2010-12-16	2010-12-25	-0.8 m/s
16	2010-12-14	2010-12-15	2010-12-25	-1.1 m/s
17	–	2010-12-19	2010-12-25	-0.9 m/s
18	–	–	2010-12-25	-1.0 m/s

**Fig. 28.** Measured power curve in a healthy state of three example wind turbines.

output to decrease. The dynamical set point made the turbine to reduce its power output even below rated power (region b and c in Fig. 25). As a consequence, the wind turbine power curve became broader. The reduction was non-constant, which made detection of the malfunction via visual observation of the power curve difficult. In Fig. 28 three example power curves during a healthy state are depicted and in Fig. 29 the power curve during controller malfunction.

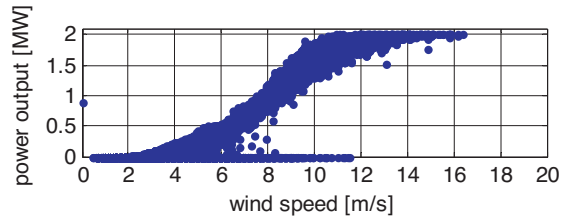
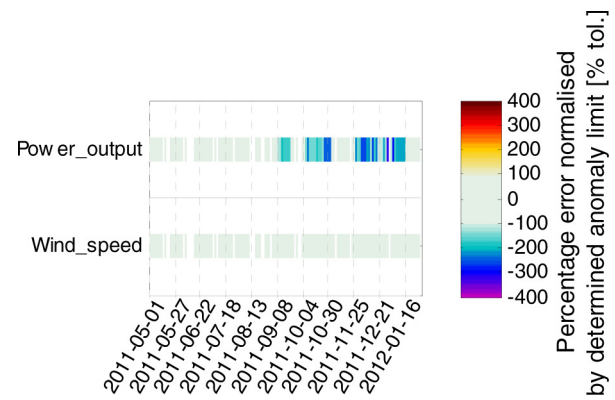
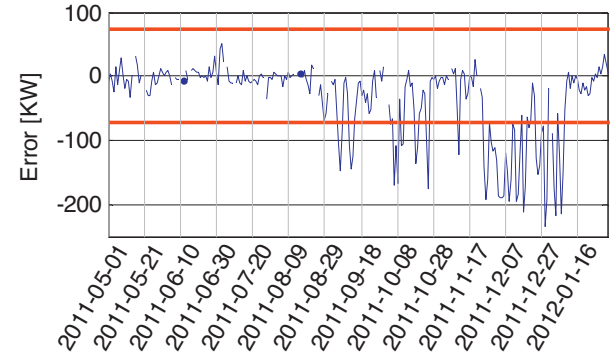
The malfunction happened after a controller software update at all WTGs. In the normalized prediction error (Fig. 30) as well as the prediction error (Fig. 31), the malfunction is clearly identifiable. Note that the inputs: ambient temperature and wind direction are not plotted in Fig. 30, as for this signals no NBM was developed.

The turbine power output is crucial for the cost of energy. It is thus of interest to monitor the turbine power output closely.

Table 11

Turbine condition evolution during turbine controller malfunction (WTG 01).

2011-09-07	2011-09-08	2011-09-13	2011-01-16
Component working as expected None	Power output too low Ambiguous	Power output too low Ambiguous	Component working as expected None

**Fig. 29.** Measured power curve during controller malfunction WTG 01.**Fig. 30.** Normalized prediction errors of the power output and related inputs (WTG 01).**Fig. 31.** Power output prediction error during controller malfunction (WTG 01).

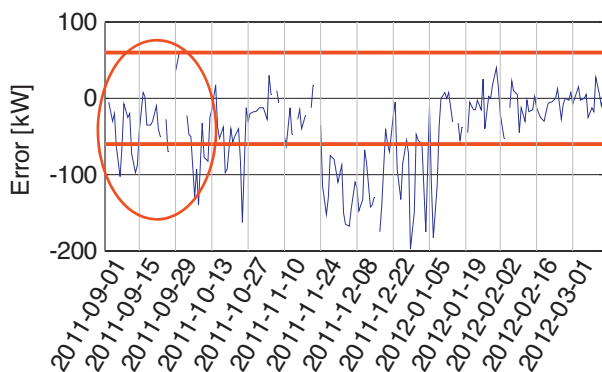
Therefore, the thresholds for the condition category “yellow” were set to ± 60 kW and “red” to ± 120 kW deviation. Based on these thresholds and the rules stated in Section 4.6, the CMS highlights the issue at the 2011-09-08. An overview about the CMS condition evaluation during the malfunction is given in Table 11. The condition evaluation at the other turbines is summarized in Table 12.

Once more for WTG 02 and WTG 18 no diagnosis was possible due to implausible wind direction signals after a controller software

Table 12

Condition evaluation summary during controller malfunction.

WTG	Yellow	Red	Issue resolved	Max div.
02	–	–	2012-01-16	-234 kW
03	2011-10-11	2011-10-25	2012-01-16	-200 kW
04	2011-08-31	2011-09-06	2012-01-16	-354 kW
05	–	2011-09-06	2012-01-16	-323 kW
06	–	2011-09-06	2012-01-16	-410 kW
07	–	2011-09-07	2012-01-16	-296 kW
08	–	2011-10-10	2012-01-16	-257 kW
09	–	2011-09-07	2012-01-16	-262 kW
10	2011-09-06	2011-09-07	2012-01-16	-287 kW
11	2011-09-12	2011-12-03	2012-01-16	-218 kW
12	2011-09-13	2011-12-03	2012-01-16	-214 kW
13	–	2011-09-07	2012-01-16	-204 kW
14	–	2011-09-07	2012-01-16	-198 kW
15	2011-09-03	2011-09-06	2012-01-16	-243 kW
16	2011-08-28	2011-09-07	2012-01-16	-241 kW
17	2011-09-12	2011-10-11	2012-01-16	-318 kW
18	–	–	2012-01-16	-244 kW

**Fig. 32.** Power output prediction error (WTG 03).

update. Dependent on the wind resource at the particular turbine location the issue is highlighted at different dates and with different condition categories. Fig. 29 shows that the power curve deviation is particularly large for wind speeds between 9 and 14 m/s. At the site and time of year the turbines do not operate in this wind speed range very often, which can cause some delay in diagnosis. However, the performance of the CMS is satisfactory, since the deviation from normal behavior in other wind speed ranges was small as indicated by the fluctuating prediction error pattern. Fig. 32 shows the prediction error for WTG 03, where the issue was detected comparably late. It can be seen that the prediction error violates the anomaly limit two times between 2011-09-01 and 2011-09-15 before it returns to its normal range again. However, currently the CMS is set up to highlight the anomaly only when the anomaly limit is violated minimum three times within seven days. Beginning of October the prediction error magnitude increases for a longer period and the issue is highlighted. This case points to the difficulty of the tradeoff between preventing false alarms and early anomaly detection.

5. Results and discussion

The results presented show that a number of different failures and malfunctions (a hydraulic oil leakage, cooling system filter pollutions, converter fan malfunctions, anemometer offsets and turbine performance decreases) can be identified using the proposed method, combining ANFIS NBM and FL. In contrast to the approach taken by Sanz-Bobi, Garcia and del Pico [4] a Full Signal ReConstruction (FSRC) model approach is used to set up the normal behavior models. In earlier research of the authors [5]

this type of models were found to detect faults earlier as well as allowing a broader anomaly spectrum to be detected. For instance with autoregressive models as proposed by Sanz-Bobi, Garcia and del Pico [4] as well as Zaher, McArthur and Infield [6] mostly relative changes in signal behavior can be detected, whereas with FSRC models as proposed by Schlechtingen and Santos [5] also absolute changes in level are detectable. In this research, the FSRC model approach has been successfully applied to a broad range of different SCADA signals, proving their ability to detect various types of relevant anomalies.

The research and advances made in the past decade (e.g. by [1,4–7]) clearly show the value of also using SCADA signals to monitor wind turbine components conditions. However, so far the focus has been on detecting faults in the gearbox and the generator. Here a CMS system has been proposed that can be successfully applied not only to detect deviation in turbine performance, but also for detection of other malfunctions at smaller components. Using FL, rules can be established which allow implementation of expert knowledge and furthermore highlight the present anomalies in the prediction error. The great advantage is that the generic rules can be established during system setup, which allows detection of present anomalies in the data, right from the beginning (after model training).

Sanz-Bobi, Garcia and del Pico [4] show in their research that the implemented rules for gearbox failure diagnosis are also valid to detect similar faults at other turbines. Using gearbox oil temperature, turbine power output and converter components NBMs in combination with FL it has been shown here that automatic analysis and diagnosis is possible also for other components and thus generalizing their result. The research further shows that in contrast to the fuzzy expert system proposed by Sanz-Bobi, Garcia and del Pico [4], which is set up to detect only positive deviations from normal behavior, it is important to extend the fuzzy expert system to also consider negative prediction error deviations as shown by the turbine performance deceases detected.

Setting up NBMs for a broad range of different signals (especially of signals used as model inputs) gives the expert full flexibility of establishing rules reducing false alarms (via a check if input signals behave normally) and identify the correct root cause. Taking into account earlier research activities of the authors [5], where based on a different data set generator stator anomalies and gearbox bearing damages were identified via FSRC NBMs, the authors are confident that also other component damages can be identified and correctly diagnosed using the proposed method.

Limitations of the method arise from limited access to sensor data. Operators currently do not have full admission to data from all sensors at their wind turbines. The more different sensor data is available, the more diverse and sophisticated models can be built and the more failures can be detected. Furthermore, the proposed system setup does not allow detection of very fast progressing faults. The chosen averaging period of one day is a trade off between model accuracy and diagnosis delay time. The system is meant for early fault detection, which is why fast progressing faults are not in focus. A CMS should allow the operator to schedule repair and take informed decisions.

6. Future aspects

With a rising number of rules, it becomes more and more important to check, if the rules established earlier still fire, when a new rule is implemented potentially interfering with the old rule. For this purpose, development of a fault reference database will be required in future, in which fault patterns are stored together with the desired diagnosis. After implementation of new rules, it should be checked, if the fuzzy expert system still gives the correct results.

With a rising number of SCADA signals, it is also required to further diversify the fuzzy expert system with regards to number of components/subsystems. In the current development there are nine component/subsystems defined. With many SCADA signals clustered in a component/subsystem problems arise, if two different anomalies or failures are present at the same time in this component. This is because the fuzzy expert application module can only give one diagnosis at a time for each component/subsystem defined. Future work will therefore require a finer diversification of different component/subsystems.

In the current development, no difference in diagnosis can be made when the same fault pattern has different root causes. To reduce the potential number of conflicts, future research will therefore focus on the implementation of other measurements, such as high resolution vibrational data or oil sample analysis in the CMS. Furthermore, turbines from a different type and brand will be included in the research.

7. Conclusions

In this paper, application examples of the CMS proposed in part one have been given. The examples show the crucial information contained in SCADA signals. Not only with respect to the component conditions, but also to the overall turbine performance. Using FSRC ANFIS NBM in combination with FL this information can be efficiently extracted. The CMS proposed supplies the basis for automated fault detection and diagnosis and aids experts in diagnosis of fault patterns. Taking into account a

large number of different SCADA signals, the architecture gives experts a large degree of freedom with respect to knowledge implementation.

Moreover, it can be concluded that rules establish with a fault experienced at one turbine can be applied to other turbines of the same type and brand to identify and diagnose similar patterns correctly. This reduces diagnosis effort required drastically and aids operators in achieving their cost reduction targets.

References

- [1] M. Schlechtingen, I.F. Santos, S. Achiche, Wind turbine condition monitoring based on SCADA data using normal behavior models. Part 1: system description, *Journal of Applied Soft Computing* (2012).
- [2] R.B. Randall, *Vibration-based Condition Monitoring*, Wiley, Chichester, West Sussex, UK, 2011, ISBN 978-0-470-74785-8.
- [3] W. Yang, J. Jiang, Wind turbine condition monitoring and reliability analysis by SCADA information, *IEEE* (2011) 1872–1875.
- [4] M.A. Sanz-Bobi, J. del Pico, M.C. Garcia, SIMAP: intelligent system for predictive maintenance application to the health condition monitoring of a windturbine gearbox, *Computers in Industry* 57 (2006) 552–568.
- [5] M. Schlechtingen, I.F. Santos, Comparative analysis of neural network and regression based condition monitoring approaches for wind turbine fault detection, *Mechanical Systems and Signal Processing* 25 (5) (2011) 1849–1875.
- [6] A. Zaher, S.D.J. McArthur, D.G. Infield, Online wind turbine fault detection through automated SCADA data analysis, *Wind Energy* 12 (2009) 574–593.
- [7] A.S. Zaher, S.D.J. McArthur, A Multi-Agent Fault Detection System for Wind Turbine Defect Recognition and Diagnosis, in: Proc. IEEE Lausanne POWERTECH, 2007, pp. 22–27.
- [8] M. Schlechtingen, I.F. Santos, S. Achiche, Using data-mining approaches for wind turbine power curve monitoring: A comparative study, *IEEE Transactions on Sustainable Energy* 4 (2013) 671–679.